Lipocalin 2 promotes inflammatory breast cancer tumorigenesis and skin invasion

Emilly S. Villodre[1,10], Xiaoding Hu[1,10], Richard Larson[2,10], Pascal Finetti[3], Kristen Gomez[4], Wintana Balema[2,10], Shane R. Stecklein[2,10], Ginette Santiago-Sanchez[5], Savitri Krishnamurthy[6,10], Juhee Song[7], Xiaoping Su[8], Naoto T. Ueno[1,10], Debu Tripathy[1,10], Steven Van Laere[9], Francois Bertucci[3], Pablo Vivas-Mejía[5], Wendy A. Woodward[2,10], Bisrat G. Debeb[1,10]

[1]Department of Breast Medical Oncology, The University of Texas MD Anderson Cancer Center, Houston, TX, USA
[2]Department of Radiation Oncology, The University of Texas MD Anderson Cancer Center, Houston, TX, USA
[3]Laboratory of Predictive Oncology, Aix-Marseille University, Inserm, CNRS, Institut Paoli-Calmettes, CRCM, Marseille, France
[4]Department of Biological Sciences, The University of Texas at Brownsville, Brownsville, TX, USA
[5]Department Biochemistry and Cancer Center, University of Puerto Rico Medical Sciences Campus San Juan, Puerto Rico
[6]Department of Pathology, The University of Texas MD Anderson Cancer Center, Houston, TX, USA
[7]Department of Biostatistics, The University of Texas MD Anderson Cancer Center, Houston, TX, USA
[8]Department of Bioinformatics and Computational Biology, The University of Texas MD Anderson Cancer Center, Houston, TX, USA
[9]Center for Oncological Research (CORE), Integrated Personalized and Precision Oncology Network (IPPON), University of Antwerp
[10]MD Anderson Morgan Welch Inflammatory Breast Cancer Clinic and Research Program, The University of Texas MD Anderson Cancer Center, Houston, TX, USA

*Corresponding author: Bisrat G. Debeb, DVM PhD, Department of Breast Medical Oncology, Section of Translational Breast Cancer Research, The Morgan Welch Inflammatory Breast Cancer Research Program and Clinic, The University of Texas MD Anderson Cancer Center, 6565 MD Anderson Blvd, Houston, TX 77030. Office phone: 713-792-0696; Lab phone: 713-795-5041; Email: bgdebeb@mdanderson.org

Abstract

Inflammatory breast cancer (IBC) is an aggressive form of primary breast cancer characterized by rapid onset and high risk of metastasis and poor clinical outcomes. The biological basis for the aggressiveness of IBC is still not well understood and no IBC-specific targeted therapies exist. In this study we report that lipocalin 2 (LCN2), a small secreted glycoprotein belonging to the lipocalin superfamily, is expressed at significantly higher levels in IBC versus non-IBC tumors, independently of molecular subtype. LCN2 levels were also significantly higher in IBC cell lines and in their culture media than in non-IBC cell lines. High expression was associated with poor-prognosis features and shorter overall survival in IBC patients. Depletion of LCN2 in IBC cell lines reduced proliferation, colony formation, migration, and cancer stem cell populations in vitro, and inhibited tumor growth, skin invasion, and brain metastasis in mouse models of IBC. Analysis of our proteomics data showed reduced expression of proteins involved in cell cycle and DNA repair in LCN2-silenced IBC cells. Our findings support that LCN2 promotes IBC tumor aggressiveness and offer a new potential therapeutic target for IBC.

Keywords: lipocalin 2, LCN2, inflammatory breast cancer, skin invasion, brain metastasis

1. Introduction

Inflammatory breast cancer (IBC) is the most aggressive and deadly variant of primary breast cancer. Although IBC is considered rare in the United States (1%-4% of all breast cancer cases), it accounts for a disproportionate 10% of breast cancer-related deaths because of its aggressive proliferation and metastasis and limited therapeutic options [1-5]. IBC disproportionately affects young and African American women [1, 6]. IBC is associated with unique clinical and biological features and a distinctive pattern of recurrence with high incidence in central nervous system, lung, and liver as first site of relapse [4, 7, 8]. Even with multimodality treatment strategies, survival rates for women with IBC are far lower than for those with other types of breast carcinoma (non-IBC), with estimated 5-year overall survival rates limited to 40% versus 63% for non-IBC [4, 6-9]. These features underscore the critical need to better define the mechanisms that drive the aggressive behavior of IBC and to develop novel agents to improve the overall prognosis for women with IBC. Efforts have been undertaken to identify pathways and therapeutic targets distinct to IBC and to better elucidate the mechanisms of IBC aggressiveness [10-15]. However, the molecular and cellular basis for IBC aggressiveness remains unclear. Identification of specific targets and unraveling the mechanisms of growth and metastasis of this aggressive disease could lead to improvements in IBC patient survival.

Lipocalin 2 (LCN2, also known as neutrophil gelatinase-associated Lipocalin [NGAL], siderocalin, or 24p3) is a 25-kDa secreted glycoprotein that belongs to the lipocalin superfamily. LCN2 is known to sequester iron, as it binds siderophore-complexed ferric iron with high affinity, and has significant roles in immune and inflammatory responses, angiogenesis, cell proliferation, survival and resistance to anticancer therapies [16-21]. LCN2 has been implicated in the progression of several types of human tumors, including breast cancer, through several mechanisms, such as stabilization of MMP-9, sequestration of iron, induction of epithelial-mesenchymal transition, apoptosis resistance, lymphangiogenesis, and cell cycle arrest [16, 17, 19-26]. Moreover, high LCN2 expression levels have been linked with poorer survival in patients

with breast cancer [17, 25, 27, 28]. Little is known regarding the oncogenic role of LCN2 in IBC tumors.

In the present study, we demonstrate that LCN2 was expressed at significantly higher levels in patients with IBC and that LCN2 promoted tumor growth, skin invasion, and metastasis in xenograft mouse models of IBC.

2. Materials and Methods

2.1. Cell lines

The SUM149 cell line was purchased from Asterand (Detroit, MI), and MDA-IBC3 cell line were generated in Dr. Woodward's lab [29, 30], and cultured in Ham's F-12 media supplemented with 10% fetal bovine serum (FBS) (GIBCO, Thermo Fisher, Carlsbad, CA), 1 µg/mL hydrocortisone (#H0888, Sigma-Aldrich, St. Louis, MO), 5 µg/mL insulin (#12585014, Thermo Fisher), and 1% antibiotic-antimycotic (#15240062, Thermo Fisher). HEK293T cells were purchased from the American Type Culture Collection (Manassas, VA, USA) and cultured in Dulbecco's modified Eagle's medium (DMEM) supplemented with 10% FBS and 1% penicillin and streptomycin (#15140122, Invitrogen, Carlsbad, CA, USA). All cell lines were kept at 37ºC in a humidified incubator with 5% CO_2 and were authenticated by short tandem repeat (STR) profiling at the Cytogenetics and Cell Authentication Core at UT MD Anderson Cancer Center.

2.2. Lentivirus-mediated knockdown

LCN2 stable knockdown clones were generated in SUM149 or MDA-IBC3 cells by using shRNA (shLCN2-1: TRCN0000060289 from Sigma-Aldrich; shLCN2-2: RHS4430-200252675 or shLCN2-3: RHS4430-200246537 from MD Anderson's Functional Genomics Core Facility. The MISSION(R) pLKO.1-puro Empty Vector (SHC001, Sigma) was used as control (shCtl). HEK293T cells were transfected with 4.05 µg of target plasmid, pCMV-VSV-G (0.45 µg; #8584, Addgene;) and pCMV delta R8.2 (3.5 µg, #12263, Addgene) by using Lipofectamine 2000 (Life

Technologies) for 24 h. SUM149 and MDA-IBC3 cells were incubated with the supernatant-containing virus plus 8 µg/mL of polybrene for 24 h. Stable cell lines were selected with 1 ug/mL of puromycin.

2.3. RNA isolation and real-time PCR

RNA was isolated by using TRIzol Reagent (Life Technologies) according to the manufacturer's instructions. The cDNA was obtained with a High Capacity cDNA Reverse Transcription Kit with RNase Inhibitor (Thermo Fisher Scientific). Real-time PCR was done by using Power SYBR Green PCR Master Mix (Applied Biosystems) on a 7500 Real-Time PCR system (Applied Biosystems, Foster City, CA). LCN2 forward primer: 3'-CCACCTCAGACCTGATCCCA-5', reverse primer: 3'- CCCCTGGAATTGGTTGTCCTG-5'; GAPDH forward primer: 3'-GAAGGTGAAGGTCGGAGT-5', reverse primer: 3'-GAAGATGGTGATGGGATTTC-5'.

2.4. ELISA

Human Lipocalin-2/NGAL Quantikine ELISA Kits (#DLCN20, R&D Systems) were used to measure the levels of LCN2 in the cell lines according to the manufacturer's instructions. Samples were assayed in duplicate.

2.5. Western blotting

Cells were lysed in RIPA buffer (Sigma) supplemented with 10 µL/mL phosphatase and 10 µL/mL protease inhibitor cocktail. SDS-PAGE and immunoblotting was carried out as described elsewhere [29]. The following primary antibodies were used: LCN2 antibody (1:1000, #MAB1757SP, R&D Systems, Minneapolis, MN, USA) or GAPDH (1:5000, #5174, Cell Signaling, Danvers, MA, USA) and samples were incubated overnight at 4ºC. Secondary antibodies (1:5000), anti-rat IgG (#HAF005, R&D Systems) and anti-rabbit IgG (#7074, Cell Signaling), were incubated with the samples for 2 h at room temperature.

97

98 *2.6. Proliferation*

99 About 2,500 cells were seeded in triplicate in a 96-well plate. Cell proliferation was measured
100 every day for up to 72 hours with the CellTiter-Blue assay (#G8080, Promega, Madison, WI)
101 according to the manufacturer's instructions. Absorbance was recorded at OD595 nm with a
102 Multifunctional Reader VICTOR X 3 (PerkinElmer, Waltham, MA).

103

104 *2.7. Colony-formation assay*

105 About 100 SUM149 or 500 MDA-IBC3 shRNA Control or LCN2-silenced cells were plated in
106 triplicate in 6-well plates. After 15 days, cells were fixed with methanol for 2 min, and stained
107 with 0.2 % (w/v) crystal violet for 30 min. Colonies were counted by using GelCount (Oxford
108 Optoronix, Abingdon, UK).

109

110 *2.8. Migration and invasion assay*

111 For the migration assay, 50,000 cells per well (triplicate) were seeded in medium without serum
112 onto 8-µm polypropylene filter inserts in Boyden chambers (Fisher). Medium with 10% FBS was
113 added onto the well. After 24 h, cells on the bottom of the filter were fixed and stained with
114 Thermo Scientific Shandon Kwik Diff Stains (Fisher). The invasion assay was done as
115 described above, except that the 8-µm polypropylene filter inserts were coated with Matrigel
116 (#CB-40234, Corning, USA) and incubated for 24 h. Ten visual fields were randomly chosen
117 under microscopy and cells were quantified by using ImageJ software (National Institutes of
118 Health, Bethesda, MD, USA).

119

120 *2.9. Mammosphere assay*

121 For primary mammosphere formation, 30,000 SUM149 or MDA-IBC3 control or LCN2
122 knockdown cells were plated in ULTRALOW attachment 6-well plates (Corning, Inc.) in

mammosphere medium (serum-free MEM supplemented with 20 ng/mL of bFGF [Gibco], 20 ng/mL epidermal growth factor [Gibco], B27 1x [Gibco], and gentamycin / penicillin / streptomycin [Thermo Fisher]). After 7 days, 5 ug/mL of MTT (Sigma-Aldrich) was added for 30 min and the mammospheres were counted by using GelCount (Oxford Optoronix). For secondary mammosphere formation, primary mammospheres were dissociated, counted, and 10,000 cells were plated in the ULTRALOW attachment 6-well plates in mammosphere media and analyzed after 7 days.

2.10. CD44/CD24 flow cytometry

About $2.5x10^5$ cells were suspended in CD24-PE mouse anti-human (#555428, BD Biosciences) or CD24-BV421 Mouse Anti-Human (#562789, BD Biosciences) and CD44-FITC mouse anti-human (#555478, BD Biosciences) or CD44-APC Mouse anti Human (#559942, BD Biosciences) solutions and incubated for 20 min on ice. Cells only, PE/BV421 only, and FITC/APC only were used as controls to set the gating. Fluorescence was detected by using a Gallios Flow Cytometer (Beckman Coulter, Brea, CA) at the Flow Cytometry and Cellular Imaging Core Facility (UT MD Anderson Cancer Center). FlowJo software (Treestar, Ashland, OR) was used to analyze the data.

2.11. Kinase Enrichment Analysis

The RPPA data was also used for the phosphoproteomic Analysis using kinase enrichment analysis (KEA - https://maayanlab.cloud/kea3/) [31]. Briefly, the 20 proteins that exhibit the highest phosphorylation fold change levels in control versus LCN2-silenced cells were analyzed. Two different analyses were performed using KEA: (1) the differentially phosphorylated proteins are queried for enrichment of kinase substrates; and (2) the differentially phosphorylated proteins are queried for enrichment of interacting proteins across 7 databases. The latter analysis is more general and is not limited to only kinase substrates. Both analyses result in the

detection of kinases that are putatively responsible for the observed phosphorylation differences. Identified proteins by both analyses were mapped onto the STRING network (https://string-db.org) to investigate their mutual interactions.

2.12. *In vivo experiments*

Four- to six-week-old female athymic SCID/Beige mice were purchased from Harlan Laboratories (Indianapolis, IN). All animal experiments were done in accordance with protocols approved by the Institutional Animal Care and Use Committee of MD Anderson Cancer Center, and mice were euthanized when they met the institutional criteria for tumor size and overall health condition. For primary tumor growth, cells were injected into the orthotopic cleared mammary fat pad of mice as previously described [32]. Briefly, $5x10^5$ SUM149 shRNA Control / LCN2 knockdown cells were injected (9 mice / Control; 10 mice / LCN2 KD). Tumor volumes were assessed weekly by measuring palpable tumors with calipers. Volume (V) was determined as V = (L x W x W) x 0.5, with L being length and W width of the tumor. To determine latency, the first day when palpable tumors appeared was used to plot the graph. For brain metastatic colonization studies, we followed our lab protocol [33]. Briefly, $1x10^6$ MDA-IBC3 GFP-labeled shRNA Control / LCN2 knockdown cells (10 mice/group) were injected via the tail vein into SCID/Beige mice. At 12 weeks after tail-vein injection, mice were euthanized, and brain tissue collected and imaged with fluorescent stereomicroscopy (SMZ1500, Nikon Instruments, Melville, NY). ImageJ was used to measure GFP-positive areas to quantify the area of brain tumor burden. For mice with more than one brain metastasis, the area of each metastasis was considered and measured.

2.13. Statistical analysis

All in vitro experiments were repeated at least three times, and graphs depict mean ± SEM. Statistical significance was determined with Student's *t* tests (unpaired, two-tailed) unless

otherwise specified. One-way analysis of variance was used for multiple comparisons. Mann-Whitney test was used when normality was not met. *LCN2* expression in breast cancer samples was analyzed in the IBC Consortium dataset [34] for IBC and from a meta-dataset previously published [35]. Tumor samples were stratified as *LCN2*-high when expression in tumor was at least 2-fold the mean expression level measured in the normal breast samples; otherwise, the sample was classified as *LCN2*-low. Kaplan-Meier curves and log-rank tests were used to compare survival distributions. Univariate and multivariate Cox regression models were used to evaluate the significance of LCN2 expression on overall survival. A p value of <0.05 was considered significant. GraphPad software (GraphPad Prism 8, La Jolla, CA) was used.

3. Results

3.1. LCN2 mRNA is highly expressed in inflammatory breast cancer

Previous studies have shown that high LCN2 expression levels were correlated with poor prognosis in breast cancer patients [17, 25-27]. We further validated these findings by analyzing a meta-dataset of 8951 breast cancers, in which 87% of tumor samples were classified as *LCN2*-low and 13% as *LCN2*-high. Table 1 summarizes the clinico-pathological patient characteristics stratified by *LCN2* expression status. High expression of *LCN2* was associated with variables commonly associated with poor outcome: younger patients' age, high grade, advanced stage tumors (pN-positive and pT3), ductal type, estrogen receptor (ER)-negative status, progesterone receptor (PR)-negative status, ERBB2-positive status, and aggressive molecular subtypes (ERBB2+ and triple-negative breast cancer [TNBC] subtypes). In this cohort, we also analyzed the association of *LCN2* expression and survival over time using the Kaplan–Meier method. We found that *LCN2*-high tumors had significantly shorter overall survival ($p<0.0001$) than *LCN2*-low tumors (Fig.1A).

Analysis of microarray data from the IBC World Consortium Dataset [34] consisting of IBC and non-IBC patient samples (n=389; IBC=137, non-IBC=252) showed that *LCN2* expression was

significantly higher in tumors from IBC patients compared to non-IBC (p=0.0003; Fig 1B). We validated this finding in another independent data set [36] that compared mRNA expression of micro dissected IBC and non-IBC tumors (p=0.0379; Fig 1C). Here too, *LCN2* expression was higher in ER-negative IBC patients compared to ER-positive (p=0.0009; Fig. 1D) and in more aggressive subtypes, ERBB2-positive and TNBC, compared to hormone receptor (HR)-positive/ERBB2-negative subtype (Fig. 1E). Multivariate analysis showed that *LCN2* was expressed significantly higher in IBC tumors relative to non-IBC tumors, independently from the molecular subtype differences (Odds ratio, 1.71, p=0.034, Table 2). Here too, the survival analysis in IBC patients showed that *LCN2*-high tumors had significantly shorter overall survival (p=0.0317) than *LCN2*-low tumors (Fig.1F). Consistent with the patient data, the levels of *LCN2* were higher in IBC cell lines (Fig. 1G) and in the supernatants collected from IBC cell lines relative to non-IBC (Fig. 1H).

Taken together, our findings show that LCN2 is highly expressed in IBC tumors and is correlated with aggressive features and poor outcome suggesting it may contribute to the aggressive pathobiology of IBC tumors.

3.2. LCN2 knockdown reduced aggressiveness features in vitro

We generated stable LCN2 knockdown cell lines [SUM149 (triple-negative IBC); MDA-IBC3 (HER2+ IBC)] to investigate the role of LCN2 in IBC aggressiveness in vitro and in vivo. LCN2 knockdown was confirmed by qRT-PCR and immunoblotting (Fig. 2A,B). Because LCN2 is a secreted protein, we evaluated levels of LCN2 protein in the supernatants from control and LCN2-silenced IBC cell lines by using ELISA. We observed significant reduction of secreted LCN2 in the LCN2-silenced IBC cells (Fig. 2C). Silencing LCN2 slightly reduced proliferation of SUM149 cells but did not affect MDA-IBC3 cells (Fig 2D). Depletion of LCN2 reduced the capacity of the cells to form colonies (Fig. 2E) and to migrate and invade (Fig. 3A,B). LCN2 silencing also significantly reduced the percentage of cancer stem cell populations in LCN2-

227 silenced IBC cells relative to control, as shown by reductions in primary and secondary
228 mammosphere formation efficiency (Fig. 3C,D) and $CD44^{+}CD24^{-}$ cell subpopulations (Fig. 3E).
229 These findings indicate that suppression of LCN2 in IBC cells reduced in vitro aggressiveness
230 features.
231
232 *3.3. Silencing of LCN2 inhibited tumor growth and skin inavsion*
233 To investigate the effects of LCN2 on tumor growth and skin invasion, key characteristics of IBC
234 tumors [4], we injected SUM149 control or LCN2-silenced cells into the cleared mammary fat
235 pad of SCID/Beige mice. Silencing of LCN2 reduced tumor volumes (p=0.0037; Fig. 4A) and
236 tumor latency, *i.e.* the ability to initiate tumor growth: mice transplanted with SUM149 LCN2-
237 silenced cells took longer to initiate tumors than did those transplanted with SUM149 control
238 cells (p=0.0145, Fig. 4B). Because IBC typically manifests with skin invasion and formation of
239 tumor emboli [4], we assessed skin invasion visually during primary tumor growth, as evidenced
240 by loss of fur at the tumor site and skin redness and thickness, and during tumor excision when
241 tumors were firmly connected with the skin. Analysis of resected tumors showed that
242 significantly fewer mice with SUM149 LCN2-silenced cells had skin invasion/recurrence
243 compared with mice implanted with control cells (shLCN2: 2 of 8 mice [25%] vs. shControl: 7 of
244 8 mice [87.5%], p=0.01; Fig. 4C;4D). On histologic examination, tumors generated from LCN2-
245 silenced cells were more differentiated than those generated from control SUM149 cells (Fig.
246 4E); we further observed tumor emboli, another hallmark of IBC tumors, in SUM149 control-
247 transplanted tumors but not in tumors generated from LCN2-silenced SUM149 cells (Fig. 4E).
248 We recently generated xenograft mouse models of brain and lung metastasis via tail-
249 vein injection of IBC cell lines [29, 33]. We also showed that sublines of SUM149 generated
250 from brain metastases (BrMS) and lung metastases (LuMS) have distinct morphologic and
251 molecular features [29]. Microarray profiling of these sublines showed upregulation of *LCN2* in
252 the brain metastatic sublines (Supplementary Fig. S1A), and we confirmed higher levels of

secreted LCN2 in the BrMS sublines versus LuMS by ELISA (Supplementary Fig. S1B). Most recently, Chi et al elegantly demonstrated that LCN2 promotes brain metastatic growth in mouse models of leptomeningeal metastasis, highlighting a potential brain metastasis-promoting role for LCN2 [37]. We investigated the functional role of LCN2 in IBC brain metastasis by using our HER2+ MDA-IBC3 mouse model, which has a high propensity to metastasize to the brain and has been used to identify targets and develop therapeutics against brain metastasis [29, 38-40]. We found that the brain metastatic burden was significantly lower in mice that had received tail-vein injection of LCN2-silenced MDA-IBC3 cells than in mice injected with control cells (Fig. 4F, p=0.0059). Also, fewer mice injected with LCN2-silenced cells developed brain metastasis (1 of 10 [10%]) than did mice injected with control cells (5 of 10 mice [50%]), although this trend was not statistically significant (p=0.1409; Fig. 4G). Representative stereofluorescence and hematoxylin and eosin images of brain metastases are shown in Fig. 4H. Overall, our findings suggest that LCN2 may drive IBC tumor progression, skin invasion/recurrence, and brain metastasis.

3.4. LCN2 silencing impairs cell cycle-associated proteins

To identify potential mechanisms and pathways involved in suppression of tumor growth and skin invasion in LCN2-silenced cells, we used reverse phase proteomics assay (RPPA) profiling to compare control and LCN2-silenced SUM149 cells. Our analysis showed reduced expression of cell cycle-associated proteins (such as AXL, FOXM1, Chk1, CDK1, Wee1, Aurora-B, and cyclin-B1 and the mTOR/AKT pathway) in LCN2-silenced IBC cells (Fig. 5A). Gene set enrichment analysis revealed several key signaling pathways that were enriched in the control cells, including those associated with cell cycling, DNA repair and mTOR signaling (Fig. 5B). Furthermore, we performed kinase enrichment analysis (KEA) [31] on the 20 proteins that exhibited the highest phosphorylation fold changes in LCN2-control vs. LCN2-silenced SUM149 cells (Supplementary Table 1). Based on the set of predicted activated kinases (Supplementary

Table 1 and Supplementary Table 2), an interaction network was generated (Fig. 5C). Based on the node degree distribution (i.e. the distribution of the number of interactions per gene in the network), MAPK1 (N=10), MAPK8 (N=7), RPS6KB1 (N=7) and MTOR (N=11) appear to be central to LCN2 action in SUM149 cells. Thus, LCN2 may regulate different pathways, including cell cycle and mTOR proteins to promote tumor growth in IBC.

4. Discussion

Inflammatory breast cancer is an aggressive form of breast cancer with poor survival outcomes. Although considerable effort has been undertaken to understand the unique biology of IBC, insights are still limited as to the molecular properties that mediate the development and aggressiveness of IBC. Herein, we report that the secreted glycoprotein LCN2 was highly expressed in tumors from IBC patients and in IBC cell lines. We further demonstrate, with in vitro and in vivo studies, that LCN2 has a tumor promoter function in IBC.

LCN2 has been implicated in the progression of several types of human tumors. LCN2 expression is higher in solid tumors than in corresponding normal tissues [24, 41], and it is mainly described as tumor promoter in many cancers, including pancreas, glioblastoma, thyroid, kidney, esophagus, and breast cancer [20, 28, 42-48].

In breast cancer, increased LCN2 expression was associated with poor outcomes and shown to be an independent prognostic marker of disease-specific-free survival [27, 48, 49]. LCN2 also correlates with several important unfavorable prognostic factors in breast cancer, such as hormone-negative status, high proliferation levels, high histologic grade, and the presence of lymph node metastases [27, 48, 49]. Further, serum levels of LCN2 have been shown to correlate with cancer progression and higher likelihood of metastasis in breast cancer [25, 50]. The oncogenic role of LCN2 has been reported in xenograft and LCN2-knockout mouse models. Disruption of the *LCN2* gene in MMTV-PyMT mice was found to suppress primary tumor formation without affecting lung metastasis [51]. Using the spontaneous MMTV-

ErbB2(V664E) LCN2$^{-/-}$ mouse model, Leng et al reported delayed tumor growth and reduced lung metastasis burden in these LCN2$^{-/-}$ mice [16]. Another group showed that injection of wild-type PyMT tumor cells into LCN2-deficient mice did not alter primary tumor formation but did significantly reduce lung metastasis [52]. LCN2 has also been shown to promote tumor progression in xenograft mouse models [17, 25]. Consistent with these studies, our current work with xenograft mouse models of IBC supports that LCN2 has a tumor promoter function in IBC tumors. We demonstrated that silencing of LCN2 reduced tumor initiation and growth, skin invasion/recurrence, and brain metastasis burden in preclinical mouse models of IBC.

We further reported that depletion of LCN2 in IBC cell cultures reduced features associated with aggressiveness in vitro, including migration, invasion, and cancer stem cell populations. Others have also found that reduction of LCN2 levels affected the same features in MDA-MB-231 cells (triple-negative breast cancer cell line) and in SK-BR-3 (HER2+ breast cancer cell line) [16, 25]. However, our data demonstrating higher levels of secreted LCN2 in IBC versus non-IBC cell lines and showing significant inhibition of key IBC tumor features such as tumor emboli/skin invasion in LCN2-silenced tumors suggest that LCN2 may exert its influence via an IBC-specific mechanism. The LCN2 protein has many functions, including transport of fatty acids and iron, induction of apoptosis, suppression of bacterial growth, and modulation of inflammatory responses [16, 17, 19-21, 25, 53]. In malignant cells, LCN2 promotes oncogenesis through several mechanisms, including stabilization of MMP-9, sequestration of iron, induction of EMT, apoptosis resistance, and regulation of cell cycling [16, 17, 19-21, 25, 53]. Here we report that LCN2 could regulate cell cycle-associated proteins such as FOXM1, Chk1, CDK1, Aurora-B, Wee1, and cyclin-B1 to promote its oncogenic role in IBC tumors. Others have also found that silencing of LCN2 affected the expression of cell cycle proteins by reducing cyclin-D1 and inducing p21, resulting in G0-G1 cell cycle arrest [22-24].

LCN2 is also a potential therapeutic target in cancer and other diseases. An antibody against LCN2 was found to decreased lung metastasis in a 4T1-induced aggressive mammary

tumor model [16]. In cervical cancer cells, treatment with LCN2-neutralizing antibody reduced the migration and invasion of cells that overexpressed LCN2 [54]. In other diseases, use of an anti-LCN2 neutralizing antibody showed reductions in reperfusion injury after stroke and attenuated skin lesions in a psoriasis mouse model [55, 56]. These findings suggest that LCN2 could be an exploitable therapeutic target in IBC and other aggressive tumors. Further studies are needed to explore therapeutic strategies in IBC models by using antibodies against LCN2 or targeting LCN2-associated molecular pathways, including those involved in cell cycling.

In summary our studies provide evidence, for the first time, that LCN2 is highly upregulated in IBC tumors and that it is required for tumor growth and skin invasion in mouse models of IBC; our findings further suggest that LCN2 could be a therapeutic target for IBC and other aggressive cancers.

Declaration of competing interest

We have no conflicts of interest to declare.

Acknowledgements

We thank Christine F. Wogan, MS, ELS, of MD Anderson's Division of Radiation Oncology for scientific editing and review of the manuscript. The Functional Genomics Core Facility at UT MD Anderson Cancer Center and the Flow Cytometry and Cellular Imaging Core Facility are both funded through NCI grant P30 CA016672 to the University of Texas MD Anderson Cancer Center.

Funding

This study was supported in part by the following grants: UPR/MDACC Partnership for Excellence in Cancer Research (U54CA096297-CA096300 to BGD), Susan G. Komen Career

Catalyst Research Grant (CCR16377813 to BGD), and State of Texas Morgan Welch Welch Inflammatory Breast Cancer Program.

Contributions

ESV and BGD conceived and designed the project, performed most of the experiments, analyzed the data, and interpreted the results. XH, RL, WB, SRS, and KG performed some experiments. PF, FB, CI, and XS helped with data analysis. JS provided statistical analysis support. SK provided pathological expertise and analysis of xenograft tumors. SVL, FB, GS, PV-M, NTU, WAW, and DT provided resources and contributed to revision of the manuscript. ESV and BGD wrote and edited the manuscript with input from all other authors.

References

[1] S. Chang, S.L. Parker, T. Pham, A.U. Buzdar, S.D. Hursting, Inflammatory breast carcinoma incidence and survival: the surveillance, epidemiology, and end results program of the National Cancer Institute, 1975-1992, Cancer, 82 (1998) 2366-2372.
[2] K.W. Hance, W.F. Anderson, S.S. Devesa, H.A. Young, P.H. Levine, Trends in inflammatory breast carcinoma incidence and survival: the surveillance, epidemiology, and end results program at the National Cancer Institute, J Natl Cancer Inst, 97 (2005) 966-975.
[3] L.Y. Dirix, P. Van Dam, A. Prove, P.B. Vermeulen, Inflammatory breast cancer: current understanding, Curr Opin Oncol, 18 (2006) 563-571.
[4] F.M. Robertson, M. Bondy, W. Yang, H. Yamauchi, S. Wiggins, S. Kamrudin, S. Krishnamurthy, H. Le-Petross, L. Bidaut, A.N. Player, S.H. Barsky, W.A. Woodward, T. Buchholz, A. Lucci, N.T. Ueno, M. Cristofanilli, Inflammatory breast cancer: the disease, the biology, the treatment, CA Cancer J Clin, 60 (2010) 351-375.
[5] Z. Wang, M. Chen, J. Pan, X. Wang, X.S. Chen, K.W. Shen, Pattern of distant metastases in inflammatory breast cancer - A large-cohort retrospective study, J Cancer, 11 (2020) 292-300.
[6] H.G. Abraham, Y. Xia, B. Mukherjee, S.D. Merajver, Incidence and survival of inflammatory breast cancer between 1973 and 2015 in the SEER database, Breast Cancer Res Treat, 185 (2021) 229-238.
[7] M. Cristofanilli, V. Valero, A.U. Buzdar, S.W. Kau, K.R. Broglio, A.M. Gonzalez-Angulo, N. Sneige, R. Islam, N.T. Ueno, T.A. Buchholz, S.E. Singletary, G.N. Hortobagyi, Inflammatory breast cancer (IBC) and patterns of recurrence: understanding the biology of a unique disease, Cancer, 110 (2007) 1436-1444.
[8] T.M. Fouad, T. Kogawa, D.D. Liu, Y. Shen, H. Masuda, R. El-Zein, W.A. Woodward, M. Chavez-MacGregor, R.H. Alvarez, B. Arun, A. Lucci, S. Krishnamurthy, G. Babiera, T.A. Buchholz, V. Valero, N.T. Ueno, Overall survival differences between patients with inflammatory and noninflammatory breast cancer presenting with distant metastasis at diagnosis, Breast Cancer Res Treat, 152 (2015) 407-416.
[9] S. Dawood, N.T. Ueno, V. Valero, W.A. Woodward, T.A. Buchholz, G.N. Hortobagyi, A.M. Gonzalez-Angulo, M. Cristofanilli, Differences in survival among women with stage III inflammatory and

noninflammatory locally advanced breast cancer appear early: a large population-based study, Cancer, 117 (2011) 1819-1826.
[10] D. Zhang, T.A. LaFortune, S. Krishnamurthy, F.J. Esteva, M. Cristofanilli, P. Liu, A. Lucci, B. Singh, M.C. Hung, G.N. Hortobagyi, N.T. Ueno, Epidermal growth factor receptor tyrosine kinase inhibitor reverses mesenchymal to epithelial phenotype and inhibits metastasis in inflammatory breast cancer, Clin Cancer Res, 15 (2009) 6639-6648.
[11] C.G. Kleer, K.L. van Golen, T. Braun, S.D. Merajver, Persistent E-cadherin expression in inflammatory breast cancer, Mod Pathol, 14 (2001) 458-464.
[12] K.L. van Golen, Z.F. Wu, X.T. Qiao, L.W. Bao, S.D. Merajver, RhoC GTPase, a novel transforming oncogene for human mammary epithelial cells that partially recapitulates the inflammatory breast cancer phenotype, Cancer Res, 60 (2000) 5832-5838.
[13] R. Costa, C.A. Santa-Maria, G. Rossi, B.A. Carneiro, Y.K. Chae, W.J. Gradishar, F.J. Giles, M. Cristofanilli, Developmental therapeutics for inflammatory breast cancer: Biology and translational directions, Oncotarget, 8 (2017) 12417-12432.
[14] X. Wang, T. Semba, L.T.H. Phi, S. Chainitikun, T. Iwase, B. Lim, N.T. Ueno, Targeting Signaling Pathways in Inflammatory Breast Cancer, Cancers (Basel), 12 (2020).
[15] E.S. Villodre, Y. Gong, X. Hu, L. Huo, E.C. Yoon, N.T. Ueno, W.A. Woodward, D. Tripathy, J. Song, B.G. Debeb, NDRG1 Expression Is an Independent Prognostic Factor in Inflammatory Breast Cancer, Cancers (Basel), 12 (2020).
[16] X. Leng, T. Ding, H. Lin, Y. Wang, L. Hu, J. Hu, B. Feig, W. Zhang, L. Pusztai, W.F. Symmans, Y. Wu, R.B. Arlinghaus, Inhibition of lipocalin 2 impairs breast tumorigenesis and metastasis, Cancer Res, 69 (2009) 8579-8584.
[17] C.A. Fernandez, L. Yan, G. Louis, J. Yang, J.L. Kutok, M.A. Moses, The matrix metalloproteinase-9/neutrophil gelatinase-associated lipocalin complex plays a role in breast tumor growth and is present in the urine of breast cancer patients, Clin Cancer Res, 11 (2005) 5390-5395.
[18] J. Yang, M.A. Moses, Lipocalin 2: a multifaceted modulator of human cancer, Cell Cycle, 8 (2009) 2347-2352.
[19] A. Iannetti, F. Pacifico, R. Acquaviva, A. Lavorgna, E. Crescenzi, C. Vascotto, G. Tell, A.M. Salzano, A. Scaloni, E. Vuttariello, G. Chiappetta, S. Formisano, A. Leonardi, The neutrophil gelatinase-associated lipocalin (NGAL), a NF-kappaB-regulated gene, is a survival factor for thyroid neoplastic cells, Proc Natl Acad Sci U S A, 105 (2008) 14058-14063.
[20] L. Leung, N. Radulovich, C.Q. Zhu, S. Organ, B. Bandarchi, M. Pintilie, C. To, D. Panchal, M.S. Tsao, Lipocalin2 promotes invasion, tumorigenicity and gemcitabine resistance in pancreatic ductal adenocarcinoma, PLoS One, 7 (2012) e46677.
[21] M. Shiiba, K. Saito, K. Fushimi, T. Ishigami, K. Shinozuka, D. Nakashima, Y. Kouzu, H. Koike, A. Kasamatsu, Y. Sakamoto, K. Ogawara, K. Uzawa, Y. Takiguchi, H. Tanzawa, Lipocalin-2 is associated with radioresistance in oral cancer and lung cancer cells, Int J Oncol, 42 (2013) 1197-1204.
[22] K.C. Chiang, T.S. Yeh, R.C. Wu, J.S. Pang, C.T. Cheng, S.Y. Wang, H.H. Juang, C.N. Yeh, Lipocalin 2 (LCN2) is a promising target for cholangiocarcinoma treatment and bile LCN2 level is a potential cholangiocarcinoma diagnostic marker, Sci Rep, 6 (2016) 36138.
[23] M.C. Tung, S.C. Hsieh, S.F. Yang, C.W. Cheng, R.T. Tsai, S.C. Wang, M.H. Huang, Y.H. Hsieh, Knockdown of lipocalin-2 suppresses the growth and invasion of prostate cancer cells, Prostate, 73 (2013) 1281-1290.
[24] J. Xu, S. Lv, W. Meng, F. Zuo, LCN2 Mediated by IL-17 Affects the Proliferation, Migration, Invasion and Cell Cycle of Gastric Cancer Cells by Targeting SLPI, Cancer Manag Res, 12 (2020) 12841-12849.
[25] J. Yang, D.R. Bielenberg, S.J. Rodig, R. Doiron, M.C. Clifton, A.L. Kung, R.K. Strong, D. Zurakowski, M.A. Moses, Lipocalin 2 promotes breast cancer progression, Proc Natl Acad Sci U S A, 106 (2009) 3913-3918.

441 [26] M. Jung, B. Oren, J. Mora, C. Mertens, S. Dziumbla, R. Popp, A. Weigert, N. Grossmann, I. Fleming, B.
442 Brune, Lipocalin 2 from macrophages stimulated by tumor cell-derived sphingosine 1-phosphate
443 promotes lymphangiogenesis and tumor metastasis, Sci Signal, 9 (2016) ra64.
444 [27] M. Bauer, J.C. Eickhoff, M.N. Gould, C. Mundhenke, N. Maass, A. Friedl, Neutrophil gelatinase-
445 associated lipocalin (NGAL) is a predictor of poor prognosis in human primary breast cancer, Breast
446 Cancer Res Treat, 108 (2008) 389-397.
447 [28] S. Candido, S.L. Abrams, L.S. Steelman, K. Lertpiriyapong, T.L. Fitzgerald, A.M. Martelli, L. Cocco, G.
448 Montalto, M. Cervello, J. Polesel, M. Libra, J.A. McCubrey, Roles of NGAL and MMP-9 in the tumor
449 microenvironment and sensitivity to targeted therapy, Biochim Biophys Acta, 1863 (2016) 438-448.
450 [29] B.G. Debeb, L. Lacerda, S. Anfossi, P. Diagaradjane, K. Chu, A. Bambhroliya, L. Huo, C. Wei, R.A.
451 Larson, A.R. Wolfe, W. Xu, D.L. Smith, L. Li, C. Ivan, P.K. Allen, W. Wu, G.A. Calin, S. Krishnamurthy, X.H.
452 Zhang, T.A. Buchholz, N.T. Ueno, J.M. Reuben, W.A. Woodward, miR-141-Mediated Regulation of Brain
453 Metastasis From Breast Cancer, J Natl Cancer Inst, 108 (2016).
454 [30] A.H. Klopp, L. Lacerda, A. Gupta, B.G. Debeb, T. Solley, L. Li, E. Spaeth, W. Xu, X. Zhang, M.T. Lewis,
455 J.M. Reuben, S. Krishnamurthy, M. Ferrari, R. Gaspar, T.A. Buchholz, M. Cristofanilli, F. Marini, M.
456 Andreeff, W.A. Woodward, Mesenchymal stem cells promote mammosphere formation and decrease E-
457 cadherin in normal and malignant breast cells, PLoS One, 5 (2010) e12180.
458 [31] A. Lachmann, A. Ma'ayan, KEA: kinase enrichment analysis, Bioinformatics, 25 (2009) 684-686.
459 [32] B.G. Debeb, L. Lacerda, W. Xu, R. Larson, T. Solley, R. Atkinson, E.P. Sulman, N.T. Ueno, S.
460 Krishnamurthy, J.M. Reuben, T.A. Buchholz, W.A. Woodward, Histone deacetylase inhibitors stimulate
461 dedifferentiation of human breast cancer cells through WNT/beta-catenin signaling, Stem Cells, 30
462 (2012) 2366-2377.
463 [33] X. Hu, E.S. Villodre, W.A. Woodward, B.G. Debeb, Modeling Brain Metastasis Via Tail-Vein Injection
464 of Inflammatory Breast Cancer Cells, J Vis Exp, (2021).
465 [34] S.J. Van Laere, N.T. Ueno, P. Finetti, P. Vermeulen, A. Lucci, F.M. Robertson, M. Marsan, T. Iwamoto,
466 S. Krishnamurthy, H. Masuda, P. van Dam, W.A. Woodward, P. Viens, M. Cristofanilli, D. Birnbaum, L.
467 Dirix, J.M. Reuben, F. Bertucci, Uncovering the molecular secrets of inflammatory breast cancer biology:
468 an integrated analysis of three distinct affymetrix gene expression datasets, Clin Cancer Res, 19 (2013)
469 4685-4696.
470 [35] F. Bertucci, P. Finetti, A. Goncalves, D. Birnbaum, The therapeutic response of ER+/HER2- breast
471 cancers differs according to the molecular Basal or Luminal subtype, NPJ Breast Cancer, 6 (2020) 8.
472 [36] W.A. Woodward, S. Krishnamurthy, H. Yamauchi, R. El-Zein, D. Ogura, E. Kitadai, S. Niwa, M.
473 Cristofanilli, P. Vermeulen, L. Dirix, P. Viens, S. van Laere, F. Bertucci, J.M. Reuben, N.T. Ueno, Genomic
474 and expression analysis of microdissected inflammatory breast cancer, Breast Cancer Res Treat, 138
475 (2013) 761-772.
476 [37] Y. Chi, J. Remsik, V. Kiseliovas, C. Derderian, U. Sener, M. Alghader, F. Saadeh, K. Nikishina, T. Bale,
477 C. Iacobuzio-Donahue, T. Thomas, D. Pe'er, L. Mazutis, A. Boire, Cancer cells deploy lipocalin-2 to collect
478 limiting iron in leptomeningeal metastasis, Science, 369 (2020) 276-282.
479 [38] E.S. Villodre, X. Hu, R. Larson, E.B. L., Y. Gong, L. Huo, J. Song, S. Krishnamurthy, N.K. Ibrahim, N.T.
480 Ueno, D. Tripathy, W.A. Woodward, B.G. debeb, Ndrg1-egfr axis in inflammatory breast cancer
481 tumorigenesis and brain metastasis [abstract], In: Proceedings of the 2019 San Antonio Breast Cancer
482 Symposium; 2019 Dec 10-14; San Antonio, TX. Philadelphia (PA): AACR Cancer Res 80 (2020).
483 [39] D.L. Smith, B.G. Debeb, H.D. Thames, W.A. Woodward, Computational Modeling of Micrometastatic
484 Breast Cancer Radiation Dose Response, Int J Radiat Oncol Biol Phys, 96 (2016) 179-187.
485 [40] K. Fukumura, P.B. Malgulwar, G.M. Fischer, X. Hu, X. Mao, X. Song, S.D. Hernandez, X.H. Zhang, J.
486 Zhang, E.R. Parra, D. Yu, B.G. Debeb, M.A. Davies, J.T. Huse, Multi-omic molecular profiling reveals
487 potentially targetable abnormalities shared across multiple histologies of brain metastasis, Acta
488 Neuropathol, 141 (2021) 303-321.

[41] S. Candido, R. Maestro, J. Polesel, A. Catania, F. Maira, S.S. Signorelli, J.A. McCubrey, M. Libra, Roles of neutrophil gelatinase-associated lipocalin (NGAL) in human cancer, Oncotarget, 5 (2014) 1576-1594.
[42] Z. Du, B. Wu, Q. Xia, Y. Zhao, L. Lin, Z. Cai, S. Wang, E. Li, L. Xu, Y. Li, H. Xu, D. Yin, LCN2-interacting proteins and their expression patterns in brain tumors, Brain Res, 1720 (2019) 146304.
[43] Z.P. Du, B.L. Wu, Y.M. Xie, Y.L. Zhang, L.D. Liao, F. Zhou, J.J. Xie, F.M. Zeng, X.E. Xu, W.K. Fang, E.M. Li, L.Y. Xu, Lipocalin 2 promotes the migration and invasion of esophageal squamous cell carcinoma cells through a novel positive feedback loop, Biochim Biophys Acta, 1853 (2015) 2240-2250.
[44] S.B. Gomez-Chou, A.K. Swidnicka-Siergiejko, N. Badi, M. Chavez-Tomar, G.B. Lesinski, T. Bekaii-Saab, M.R. Farren, T.A. Mace, C. Schmidt, Y. Liu, D. Deng, R.F. Hwang, L. Zhou, T. Moore, D. Chatterjee, H. Wang, X. Leng, R.B. Arlinghaus, C.D. Logsdon, Z. Cruz-Monserrate, Lipocalin-2 Promotes Pancreatic Ductal Adenocarcinoma by Regulating Inflammation in the Tumor Microenvironment, Cancer Res, 77 (2017) 2647-2660.
[45] M. Miki, T. Oono, N. Fujimori, T. Takaoka, K. Kawabe, Y. Miyasaka, T. Ohtsuka, D. Saito, M. Nakamura, Y. Ohkawa, Y. Oda, M. Suyama, T. Ito, Y. Ogawa, CLEC3A, MMP7, and LCN2 as novel markers for predicting recurrence in resected G1 and G2 pancreatic neuroendocrine tumors, Cancer Med, 8 (2019) 3748-3760.
[46] G.S. Santiago-Sanchez, V. Pita-Grisanti, B. Quinones-Diaz, K. Gumpper, Z. Cruz-Monserrate, P.E. Vivas-Mejia, Biological Functions and Therapeutic Potential of Lipocalin 2 in Cancer, Int J Mol Sci, 21 (2020).
[47] A. Viau, K. El Karoui, D. Laouari, M. Burtin, C. Nguyen, K. Mori, E. Pillebout, T. Berger, T.W. Mak, B. Knebelmann, G. Friedlander, J. Barasch, F. Terzi, Lipocalin 2 is essential for chronic kidney disease progression in mice and humans, J Clin Invest, 120 (2010) 4065-4076.
[48] A.S. Wenners, K. Mehta, S. Loibl, H. Park, B. Mueller, N. Arnold, S. Hamann, J. Weimer, B. Ataseven, S. Darb-Esfahani, C. Schem, C. Mundhenke, F. Khandan, C. Thomssen, W. Jonat, H.J. Holzhausen, G. von Minckwitz, C. Denkert, M. Bauer, Neutrophil gelatinase-associated lipocalin (NGAL) predicts response to neoadjuvant chemotherapy and clinical outcome in primary human breast cancer, PLoS One, 7 (2012) e45826.
[49] S.P. Stoesz, A. Friedl, J.D. Haag, M.J. Lindstrom, G.M. Clark, M.N. Gould, Heterogeneous expression of the lipocalin NGAL in primary breast cancers, Int J Cancer, 79 (1998) 565-572.
[50] X. Provatopoulou, A. Gounaris, E. Kalogera, F. Zagouri, I. Flessas, E. Goussetis, A. Nonni, I. Papassotiriou, G. Zografos, Circulating levels of matrix metalloproteinase-9 (MMP-9), neutrophil gelatinase-associated lipocalin (NGAL) and their complex MMP-9/NGAL in breast cancer disease, BMC Cancer, 9 (2009) 390.
[51] T. Berger, C.C. Cheung, A.J. Elia, T.W. Mak, Disruption of the Lcn2 gene in mice suppresses primary mammary tumor formation but does not decrease lung metastasis, Proc Natl Acad Sci U S A, 107 (2010) 2995-3000.
[52] B. Oren, J. Urosevic, C. Mertens, J. Mora, M. Guiu, R.R. Gomis, A. Weigert, T. Schmid, S. Grein, B. Brune, M. Jung, Tumour stroma-derived lipocalin-2 promotes breast cancer metastasis, J Pathol, 239 (2016) 274-285.
[53] C. Hu, K. Yang, M. Li, W. Huang, F. Zhang, H. Wang, Lipocalin 2: a potential therapeutic target for breast cancer metastasis, Onco Targets Ther, 11 (2018) 8099-8106.
[54] I.H. Chung, T.I. Wu, C.J. Liao, J.Y. Hu, Y.H. Lin, P.J. Tai, C.H. Lai, K.H. Lin, Overexpression of lipocalin 2 in human cervical cancer enhances tumor invasion, Oncotarget, 7 (2016) 11113-11126.
[55] G. Wang, Y.C. Weng, I.C. Chiang, Y.T. Huang, Y.C. Liao, Y.C. Chen, C.Y. Kao, Y.L. Liu, T.H. Lee, W.H. Chou, Neutralization of Lipocalin-2 Diminishes Stroke-Reperfusion Injury, Int J Mol Sci, 21 (2020).
[56] S. Shao, T. Cao, L. Jin, B. Li, H. Fang, J. Zhang, Y. Zhang, J. Hu, G. Wang, Increased Lipocalin-2 Contributes to the Pathogenesis of Psoriasis by Modulating Neutrophil Chemotaxis and Cytokine Secretion, J Invest Dermatol, 136 (2016) 1418-1428.

Figure Legends

Fig. 1 LCN2 was highly expressed in tumors from patients with IBC. **(A)** High *LCN2* expression was associated with shorter overall survival in a meta-dataset of patients with non-IBC. **(B-C)** *LCN2* mRNA expression was higher in tumors from IBC patients versus non-IBC patients in two independent breast cancer datasets [34, 36]. **(D)** *LCN2* mRNA expression was higher in estrogen receptor (ER)-negative compared to ER+ samples IBC samples. **(E)** *LCN2* mRNA expression was higher in more aggressive molecular subtypes, ERBB2+ and triple-negative breast cancer (TNBC) , compared to hormone receptor (HR)-positive/HERBB2-negative subtype. **(F)** *LCN2*-high expression correlates with shorter overall survival in patients with IBC. **(G)** *LCN2* mRNA expression was higher in IBC cell lines compared to non-IBC cell lines. **(H-I)** LCN2 protein expression was higher in IBC cell lines compared to non-IBC cell lines shown by **(H)** immunoblotting or **(I)** ELISA for secreted LCN2 in supernatants. Graphpad Prism software was used to obtain the *p* values, with Mann-Whitney tests used to compare two categories or one-way analysis of variance to compare three or more categories.

Fig. 2 Silencing LCN2 decreased colony formation efficiency. LCN2 was knocked down (shLCN2) in two IBC cell lines (SUM149 and MDA-IBC3) and confirmed by **(A)** qRT-PCR and **(B)** immunoblotting. **(C)** Secreted LCN2 measured in control and silenced cells by ELISA at the indicated times. **(D)** Proliferation was evaluated in control and LCN2-silenced SUM149 and MDA-IBC3 cells with CellTiterBlue assay on the indicated days. **(E)** Cells were seeded in low numbers to measure the capacity to form colonies in LCN2 knockdown and control.

Fig. 3. **LCN2 knockdown reduced aggressiveness features in vitro. (A)** Migration and **(B)** invasion by control cells (shCtl) and LCN2-knockdown (shLCN2) SUM149 cells. **(C)** Primary

562 mammosphere formation efficiency and **(D)** secondary mammosphere formation efficiency. **(E)**
563 $CD44^{+}CD24^{-}$ cells (marker of cancer stem cells) were measured by flow cytometry.
564
565 **Fig. 4. Silencing LCN2 inhibited tumor growth and skin inavsion. (A-C)** SUM149 shRNA Ctl
566 or LCN2-knockdown (shLCN2) cells were transplanted orthotopically into the cleared mammary
567 fat pad of SCID/Beige mice (n= 9/Ctl; 10/shLCN2) and tumor volume measured weekly; **(A)**
568 tumor volume, **(B)** tumor latency, and **(C)** incidence of skin invasion/recurrence after resection
569 of primary tumors. **(D-E)** Hematoxylin and eosin staining of primary tumors generated from
570 LCN2 control and knockdown SUM149 cells. Both **(D)** skin invasion and **(E)** tumor emboli, two
571 hallmarks of IBC, appeared only in the control-derived tumors (arrow head). Scale bar, 100 µm.
572 **(F)** Metastatic burden (area) of each brain metastasis formed was quantified by using ImageJ
573 software. BM, brain metastasis. **(G)** Incidence of brain metastasis. N=10 mice per group.
574 Fisher's exact test was used to obtain *p* values. **(H)** Top, green fluorescent protein (GFP)
575 imaging of brain metastasis lesions generated from tail-vein injection of GFP-labeled MDA-IBC3
576 shRNA Ctl or LCN2 knockdown cells, and bottom, hematoxylin and eosin stains of brain
577 metastasis lesions. Scale bar, 50 µm.
578
579 **Fig. 5. Silencing of LCN2 impairs cell cycle-associated proteins. (A)** The top proteins
580 downregulated in LCN2-silenced cells compared with control cells after reverse phase protein
581 array (RPPA) proteomic analysis. **(B)** Gene set enrichment analysis of RPPA data identified
582 pathways that are enriched or downregulated in control vs. LCN2-silenced SUM149 cells. **(C)**
583 STRING interaction network of predicted active kinases based on enrichment of kinase
584 substrates and protein interactions identified using kinase enrichment analysis. The confidence
585 of the interaction is reflected by the edge thickness. Based on node distribution analysis, four
586 central proteins were identified (MAPK1, MAPK8, RPS6KB1 and MTOR).
587

588 **Table 1.** Clinico-pathological characteristics of tumor samples from patients with IBC or non-IBC
589 according to *LCN2* expression.
590
591 **Table 2.** Univariate and multivariate Cox regression analysis of samples from 389 patients with
592 inflammatory breast cancer (IBC) or non-IBC.
593
594 **Additional file 1. Figure S1.** LCN2 expression is higher in sublines generated from brain
595 metastasis (BrMS) than those generated from lung metastasis (LuMS). **(A)** Microarray analysis
596 of sublines generated from BrMS or LuMS of SUM149 cells showed *LCN2* to be one of the top
597 upregulated genes in BrMS (red arrow). Samples are described in Debeb 2016 [29]. **(B)** LCN2
598 is secreted in higher levels in BrMS versus LuMS.
599
600 **Additional file 2. Supplementary Table 1.** Top kinases predicted to be activated based on
601 kinase-substrate interactions of differentially phosphorylated proteins.
602
603 **Additional file 3. Supplementary Table 2.** Top kinases predicted to be activated based on
604 kinase-substrate and protein-protein interaction analysis of differentially phosphorylated proteins
605 across 10 different knowledge bases.

Figure 1

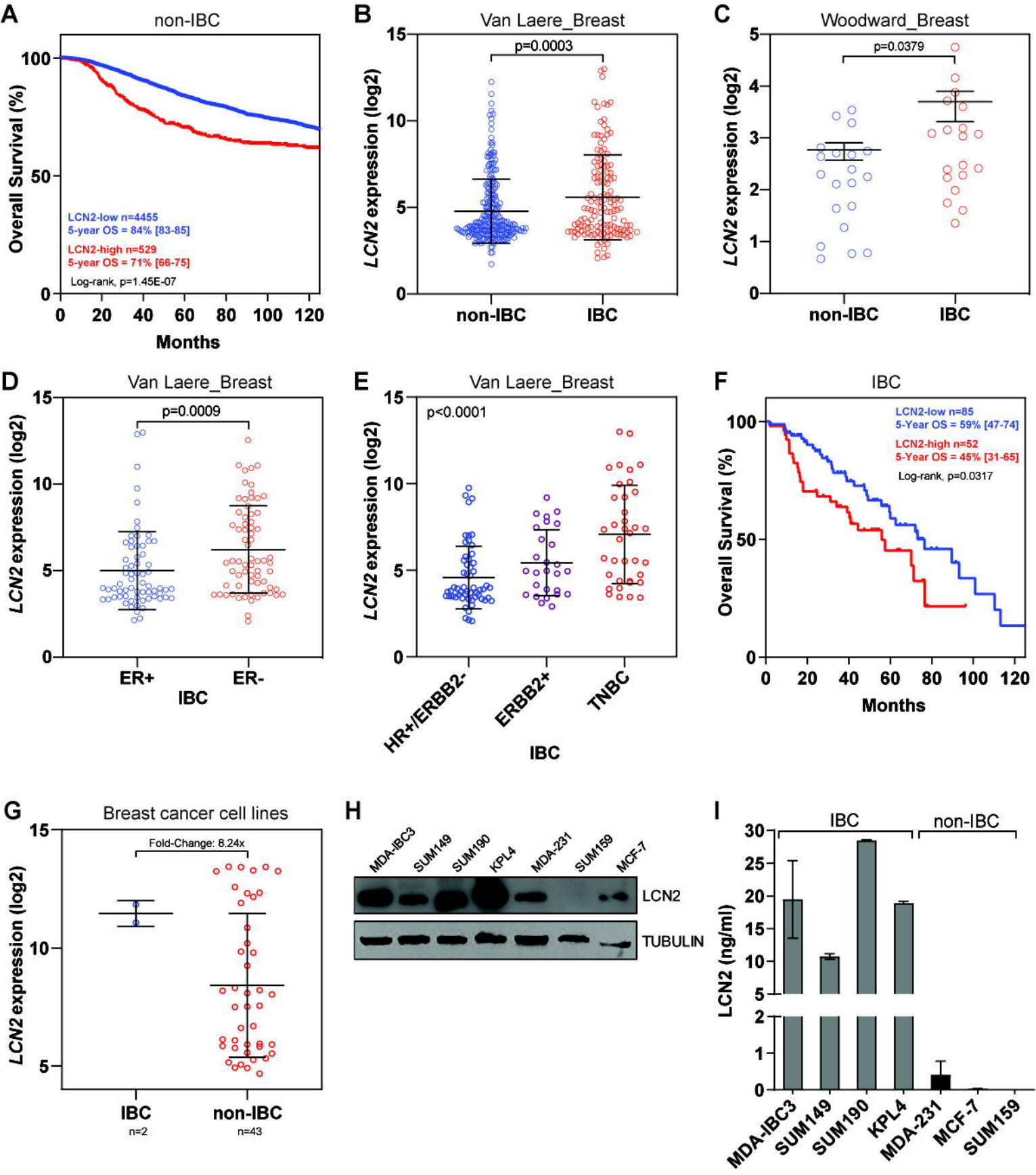
A
non-IBC
Overall Survival (%)
LCN2-low n=4455
5-year OS = 84% [83-85]
LCN2-high n=529
5-year OS = 71% [66-75]
Log-rank, p=1.45E-07
Months
B
Van Laere_Breast
p=0.0003
LCN2 expression (log2)
non-IBC
IBC
C
Woodward_Breast
p=0.0379
LCN2 expression (log2)
non-IBC
IBC
D
Van Laere_Breast
p=0.0009
LCN2 expression (log2)
ER+
ER-
IBC
E
Van Laere_Breast
p<0.0001
LCN2 expression (log2)
HR+/ERBB2-
ERBB2+
TNBC
IBC
F
IBC
LCN2-low n=85
5-Year OS = 59% [47-74]
LCN2-high n=52
5-Year OS = 45% [31-65]
Log-rank, p=0.0317
Overall Survival (%)
Months
G
Breast cancer cell lines
Fold-Change: 8.24x
LCN2 expression (log2)
IBC
n=2
non-IBC
n=43
H
MDA-IBC3
SUM149
SUM190
KPL4
MDA-231
SUM159
MCF-7
LCN2
TUBULIN
I
IBC
non-IBC
LCN2 (ng/ml)
MDA-IBC3
SUM149
SUM190
KPL4
MDA-231
MCF-7
SUM159

Figure 2

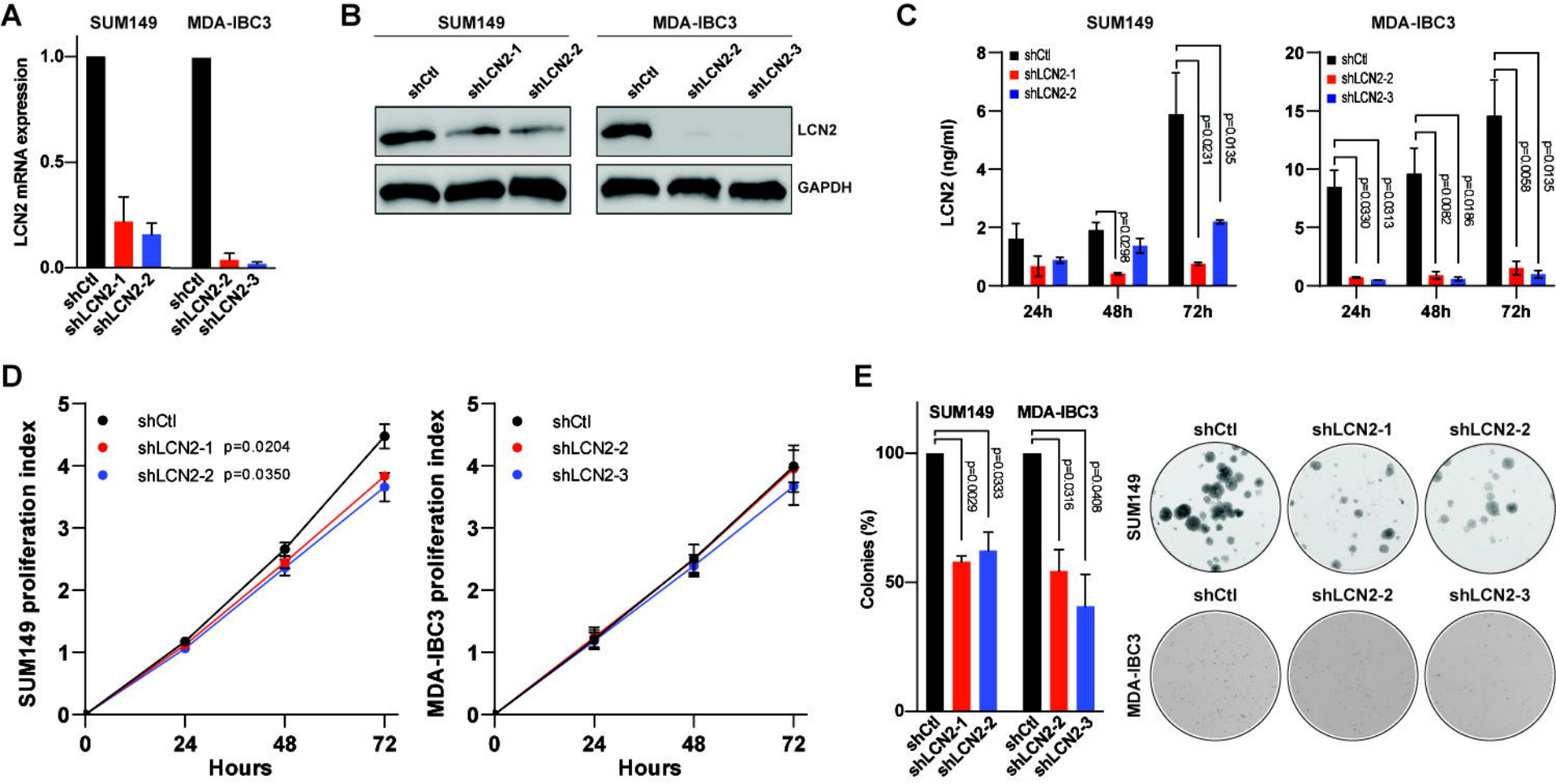
A
SUM149
MDA-IBC3
LCN2 mRNA expression
1.0
0.5
0.0
shCtl
shLCN2-1
shLCN2-2
shCtl
shLCN2-2
shLCN2-3
B
SUM149
MDA-IBC3
shCtl
shLCN2-1
shLCN2-2
shCtl
shLCN2-2
shLCN2-3
LCN2
GAPDH
C
SUM149
MDA-IBC3
LCN2 (ng/ml)
shCtl
shLCN2-1
shLCN2-2
shLCN2-3
p=0.0298
p=0.0231
p=0.0135
p=0.0330
p=0.0313
p=0.0082
p=0.0186
p=0.0058
p=0.0135
24h
48h
72h
D
SUM149 proliferation index
MDA-IBC3 proliferation index
shCtl
shLCN2-1 p=0.0204
shLCN2-2 p=0.0350
shLCN2-3
Hours
E
SUM149
MDA-IBC3
Colonies (%)
p=0.0029
p=0.0333
p=0.0316
p=0.0408
shCtl
shLCN2-1
shLCN2-2
shCtl
shLCN2-2
shLCN2-3

Figure 3

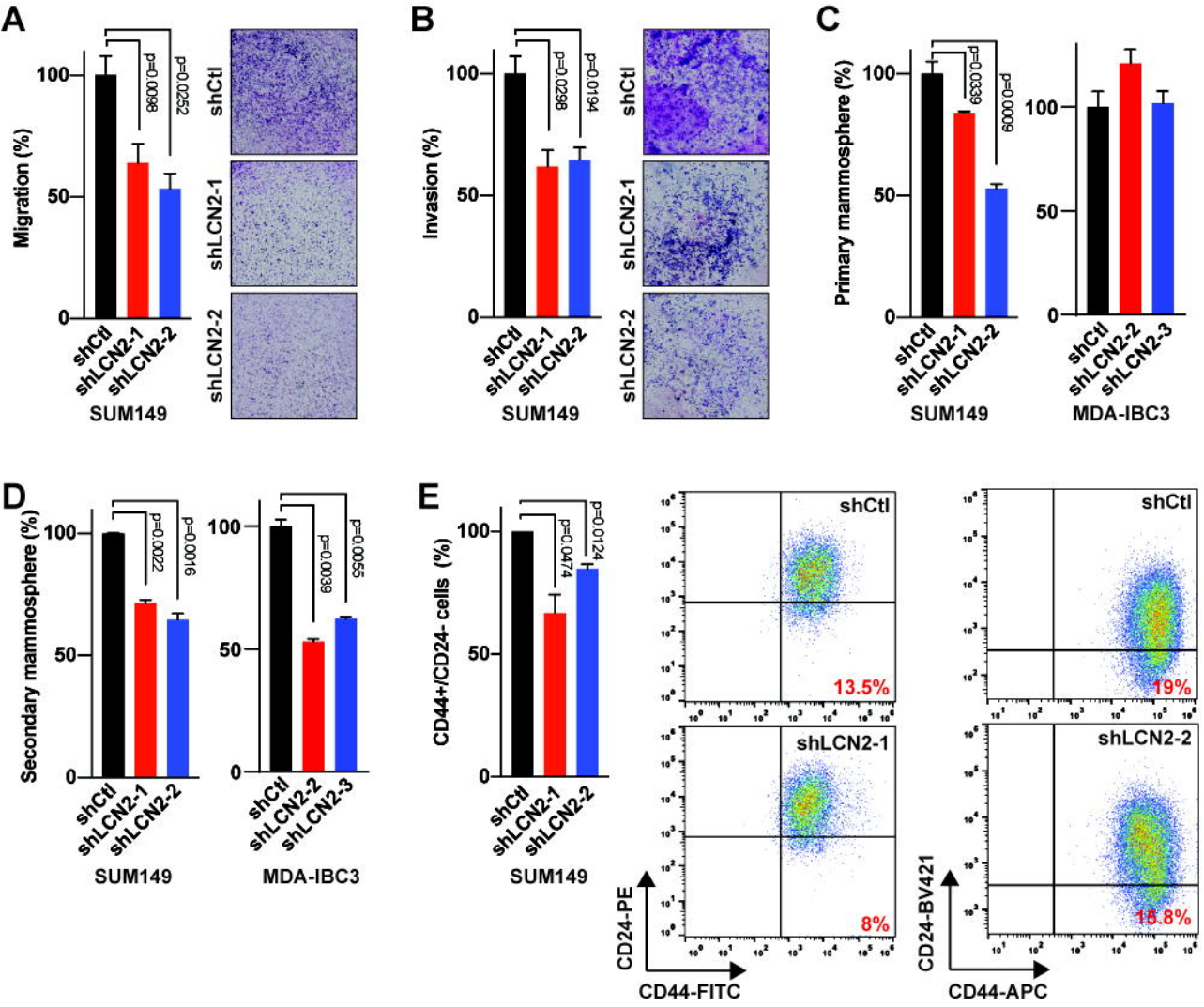
A
Migration (%)
100
50
0
p=0.0252
p=0.0098
shCtl
shLCN2-1
shLCN2-2
SUM149
shCtl
shLCN2-1
shLCN2-2
B
Invasion (%)
p=0.0194
p=0.0298
SUM149
C
Primary mammosphere (%)
p=0.0009
p=0.0339
SUM149
MDA-IBC3
shCtl
shLCN2-2
shLCN2-3
D
Secondary mammosphere (%)
p=0.0016
p=0.0022
p=0.0055
p=0.0039
E
CD44+/CD24- cells (%)
p=0.0124
p=0.0474
13.5%
19%
8%
18.8%
CD24-PE
CD44-FITC
CD24-BV421
CD44-APC

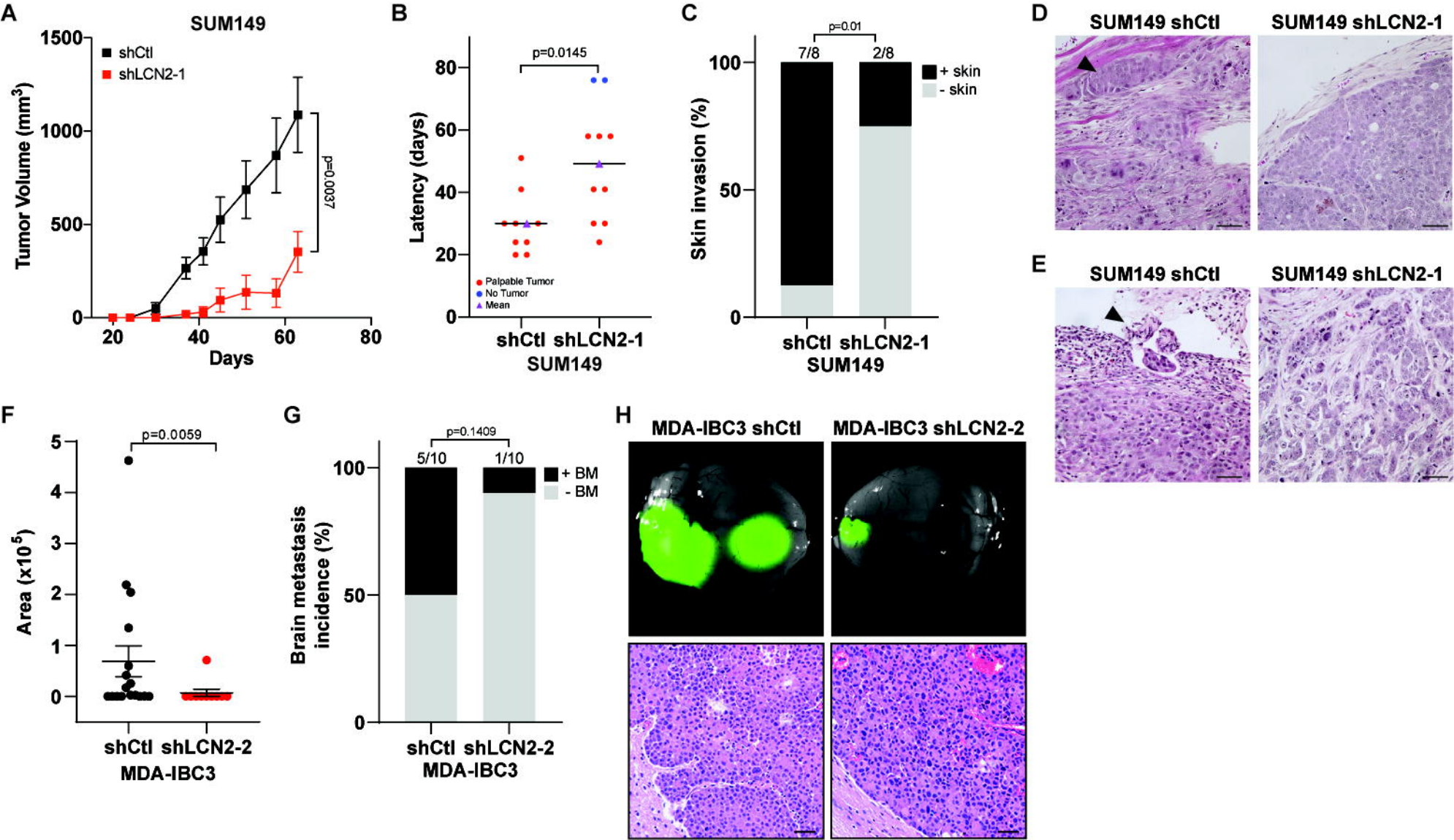
A
SUM149
shCtl
shLCN2-1
Tumor Volume (mm3)
Days
p=0.0037
B
p=0.0145
Latency (days)
Palpable Tumor
No Tumor
Mean
shCtl shLCN2-1
SUM149
C
p=0.01
7/8
2/8
+ skin
- skin
Skin invasion (%)
shCtl shLCN2-1
SUM149
D
SUM149 shCtl
SUM149 shLCN2-1
E
SUM149 shCtl
SUM149 shLCN2-1
F
p=0.0059
Area (x10^5)
shCtl shLCN2-2
MDA-IBC3
G
p=0.1409
5/10
1/10
+ BM
- BM
Brain metastasis incidence (%)
shCtl shLCN2-2
MDA-IBC3
H
MDA-IBC3 shCtl
MDA-IBC3 shLCN2-2

Figure 5

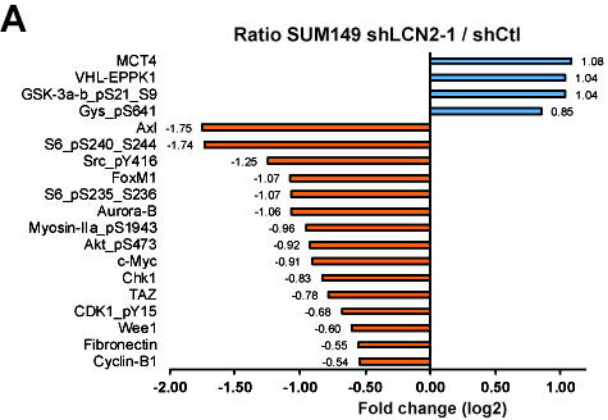
A
Ratio SUM149 shLCN2-1 / shCtl
MCT4 1.08
VHL-EPPK1 1.04
GSK-3a-b_pS21_S9 1.04
Gys_pS641 0.85
Axl -1.75
S6_pS240_S244 -1.74
Src_pY416 -1.25
FoxM1 -1.07
S6_pS235_S236 -1.07
Aurora-B -1.06
Myosin-IIa_pS1943 -0.96
Akt_pS473 -0.92
c-Myc -0.91
Chk1 -0.83
TAZ -0.78
CDK1_pY15 -0.68
Wee1 -0.60
Fibronectin -0.55
Cyclin-B1 -0.54
-2.00 -1.50 -1.00 -0.50 0.00 0.50 1.00
Fold change (log2)

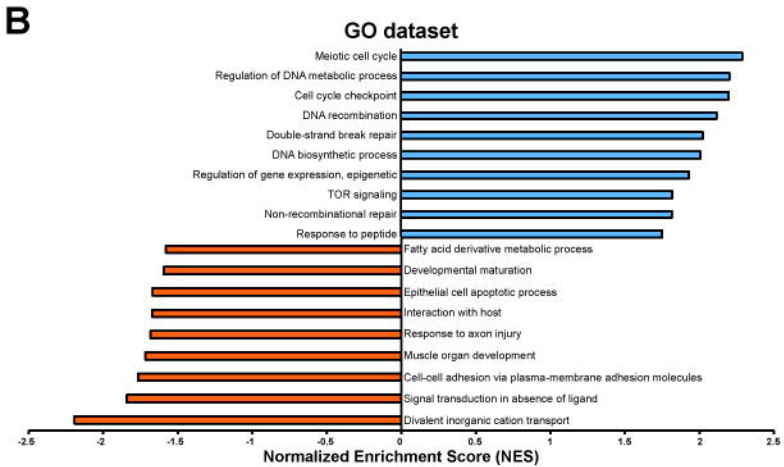
B
GO dataset
Meiotic cell cycle
Regulation of DNA metabolic process
Cell cycle checkpoint
DNA recombination
Double-strand break repair
DNA biosynthetic process
Regulation of gene expression, epigenetic
TOR signaling
Non-recombinational repair
Response to peptide
Fatty acid derivative metabolic process
Developmental maturation
Epithelial cell apoptotic process
Interaction with host
Response to axon injury
Muscle organ development
Cell-cell adhesion via plasma-membrane adhesion molecules
Signal transduction in absence of ligand
Divalent inorganic cation transport
-2.5 -2 -1.5 -1 -0.5 0 0.5 1 1.5 2 2.5
Normalized Enrichment Score (NES)

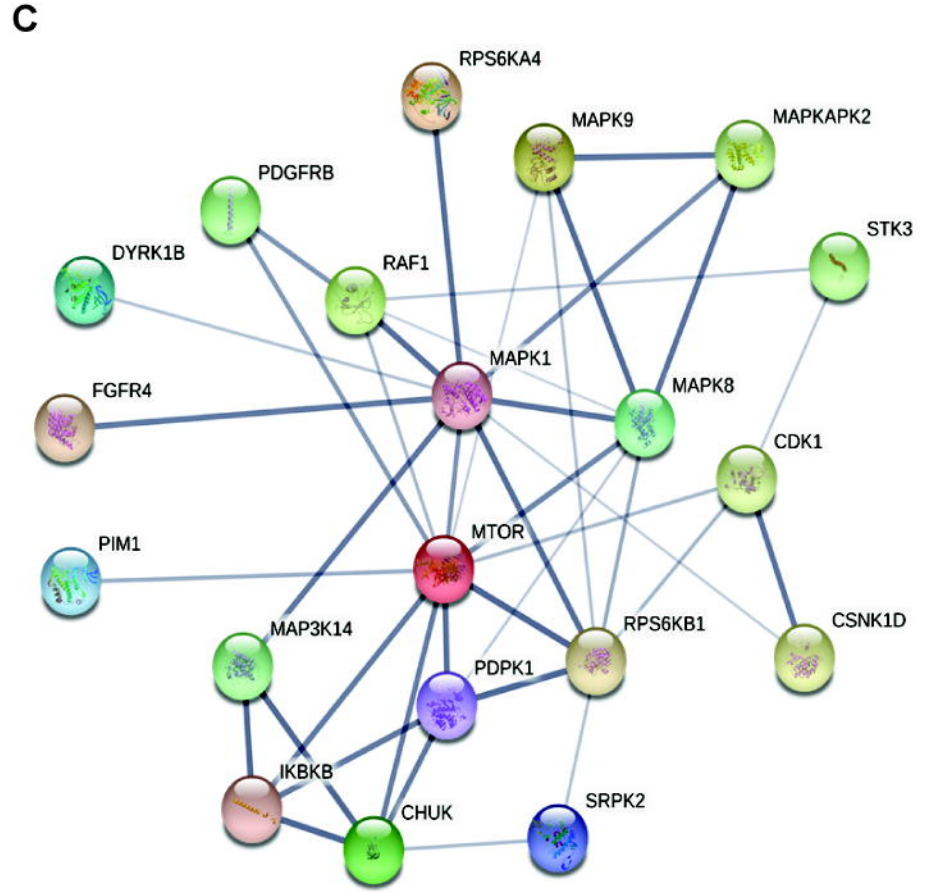
C
RPS6KA4
MAPK9
MAPKAPK2
PDGFRB
STK3
DYRK1B
RAF1
MAPK1
MAPK8
FGFR4
CDK1
PIM1
MTOR
MAP3K14
RPS6KB1
CSNK1D
PDPK1
IKBKB
CHUK
SRPK2

Table 1
Clinico-pathological characteristics of tumor samples from patients with inflammatory breast cancer (IBC) or non-IBC according to *LCN2* expression.

Covariate	Level	N	*LCN2*-low	*LCN2*-high	*p*-value
Age (years)	≤50	2587	2218 (36%)	369 (42%)	1.10E-04
	>50	4520	4018 (64%)	502 (58%)	
Pathological Grade	1	717	680 (13%)	37 (4%)	<1.00E-06
	2	2549	2359 (43%)	190 (22%)	
	3	3016	2389 (44%)	627 (73%)	
Pathological Node (pN)	Negative	3666	3253 (57%)	413 (53%)	3.89E-02
	Positive	2788	2426 (43%)	362 (47%)	
Pathological Size (pT)	pT1	2116	1912 (38%)	204 (31%)	2.00E-06
	pT2	2931	2588 (52%)	343 (53%)	
	pT3	604	498 (10%)	106 (16%)	
Pathological type	Ductal	4027	3492 (78%)	535 (86%)	3.00E-06
	Lobular	500	471 (11%)	29 (5%)	
	Other	574	519 (12%)	55 (9%)	
Estrogen Receptor status[1]	Negative	2753	1955 (25%)	798 (71%)	1.97E-215
	Positive	6198	5875 (75%)	323 (29%)	
Progesterone Receptor status[1]	Negative	4635	3746 (48%)	889 (80%)	3.06E-86
	Positive	4284	4055 (52%)	229 (20%)	
ERBB2 status[1]	Negative	7862	6975 (89%)	887 (79%)	2.37E-21
	Positive	1089	855 (11%)	234 (21%)	
Hormone Receptor subtype[1]	HR+/ERBB2-	5914	5598 (72%)	316 (28%)	<1.00E-06
	ERBB2+	1089	855 (11%)	234 (21%)	
	TNBC	1938	1368 (17%)	570 (51%)	
Overall Survival[2]		4984	1.00	1.58 [1.34 - 1.86][3]	3.31E-08

[1]mRNA status; [2]Univariate analysis; [3]hazard ratio (95% confidence interval)
Abbreviations: HR, hormone receptor; ERBB2, Erb-B2 Receptor Tyrosine Kinase 2 (HER2); TNBC, triple-negative breast cancer

Table 2
Univariate and multivariate Cox regression analysis of inflammatory breast cancer (IBC) patient samples versus non-IBC (n=389).

	Univariate			Multivariate		
IBC vs. non-IBC	**Odds-ratio**	**95% CI**	**p-value**	**Odds-ratio**	**95% CI**	**p-value**
LCN2, high vs low	2.09	1.43 - 3.06	1.43E-03	1.71	1.13 - 2.6	3.42E-02
Molecular subtype						
ERBB2+ vs HR+/ERBB2-	2.82	1.82 - 4.38	1.02E-04	2.5	1.59 - 3.93	8.16E-04
TNBC vs HR+/ERBB2-	1.9	1.22 - 2.97	1.69E-02	1.51	0.93 - 2.44	0.162

Abbreviations: HR, hormone receptor; ERBB2, Erb-B2 Receptor Tyrosine Kinase 2 (HER2); TNBC, triple-negative breast cancer